Molecular Vision 2015; 21:515-522 <http://www.molvis.org/molvis/v21/515>
Received 19 January 2015 | Accepted 29 April 2015 | Published 1 May 2015

Optical coherence tomography enables imaging of tumor initiation in the TAg-RB mouse model of retinoblastoma

Andrea A. Wenzel,[1] Michael N. O'Hare,[1,2] Mehdi Shadmand,[1] Timothy W. Corson[1,3,4,5]

[1]Eugene and Marilyn Glick Eye Institute, Department of Ophthalmology, Indiana University School of Medicine, Indianapolis, IN; [2]School of Biomedical Science, University of Ulster, Coleraine, Northern Ireland, UK; [3]Department of Biochemistry and Molecular Biology, Indiana University School of Medicine, Indianapolis, IN; [4]Department of Pharmacology and Toxicology, Indiana University School of Medicine, Indianapolis, IN; [5]Indiana University Melvin and Bren Simon Cancer Center, Indianapolis, IN

Purpose: Retinoblastoma is the most common primary intraocular malignancy in children. Although significant advances in treatment have decreased mortality in recent years, morbidity continues to be associated with these therapies, and therefore, there is a pressing need for new therapeutic options. Transgenic mouse models are popular for testing new therapeutics as well as studying the pathophysiology of retinoblastoma. The T-antigen retinoblastoma (TAg-RB) model has close molecular and histological resemblance to human retinoblastoma tumors; these mice inactivate pRB by retinal-specific expression of the Simian Virus 40 T-antigens. Here, we evaluated whether optical coherence tomography (OCT) imaging could be used to document tumor growth in the TAg-RB model from the earliest stages of tumor development.
Methods: The Micron III rodent imaging system was used to obtain fundus photographs and OCT images of both eyes of TAg-RB mice weekly from 2 to 12 weeks of age and at 16 and 20 weeks of age to document tumor development. Tumor morphology was confirmed with histological analysis.
Results: Before being visible on funduscopy, hyperreflective masses arising in the inner nuclear layer were evident at 2 weeks of age with OCT imaging. After most of these hyperreflective cell clusters disappeared around 4 weeks of age, the first tumors became visible on OCT and funduscopy by 6 weeks. The masses grew into discrete, discoid tumors, preferentially in the periphery, that developed more irregular morphology over time, eventually merging and displacing the inner retinal layers into the vitreous.
Conclusions: OCT is a non-invasive imaging modality for tracking early TAg-RB tumor growth in vivo. Using OCT, we characterized TAg-positive cells as early as 2 weeks, corresponding to the earliest stages at which tumors are histologically evident, and well before they are evident with funduscopy. Tracking tumor growth from its earliest stages will allow better analysis of the efficacy of novel therapeutics and genetic factors tested in this powerful mouse model.

Combined therapeutic modalities for retinoblastoma have significantly reduced the mortality associated with this disease. Currently, close to 95% of children with retinoblastoma in the developed world are cured of their primary tumor [1]. Despite advances in treatment, significant morbidity associated with this cancer remains, including loss of vision or enucleation. New therapeutic options are therefore being investigated. In the clinic, there is a focus on novel delivery routes such as intravitreal and intraarterial chemotherapies [2-4], while preclinical scientists are developing targeted therapies [5-8]. Animal models are used to further understand retinoblastoma tumorigenesis, as well as monitor response to experimental treatments [9].

Of these animal models, transgenic mouse models can be used to test new therapeutics and study the developmental pathophysiology of retinoblastoma. One such transgenic model, the T-antigen retinoblastoma (TAg-RB) model [10], has a molecular and histological resemblance to human retinoblastoma tumors [11]. In human retinoblastoma, the retinoblastoma gene, *RB1* (GeneID: 5925, OMIM: 614041), is almost always [12] inactivated by mutation, leading to loss of function of the retinoblastoma protein, pRB [13-15]. In TAg-RB mice, pRB is inactivated by retinal-specific expression of the Simian Virus 40 T-antigens [10]. The Simian Virus 40 large T antigen (TAg) provides a biochemical means of functionally knocking out pRB family members, along with p53 and other protein targets [16], and has been used to drive various mouse tumor models [17]. Similar to the human retinoblastoma, TAg-RB tumors contain Homer Wright rosettes and are the only murine retinoblastoma tumors reported to show Flexner-Wintersteiner rosettes [10]. The presence of both types of rosette is pathognomonic of human retinoblastoma [18]. Moreover, molecular analyses of TAg-RB tumors have indicated that these tumors recapitulate several of the gene expression changes documented in

Correspondence to: Timothy W. Corson, Indiana University School of Medicine, Ophthalmology, 1160 W Michigan St, Indianapolis, IN 46202; Phone: (317) 274-3305; FAX: (317) 274-2277; email: tcorson@iupui.edu

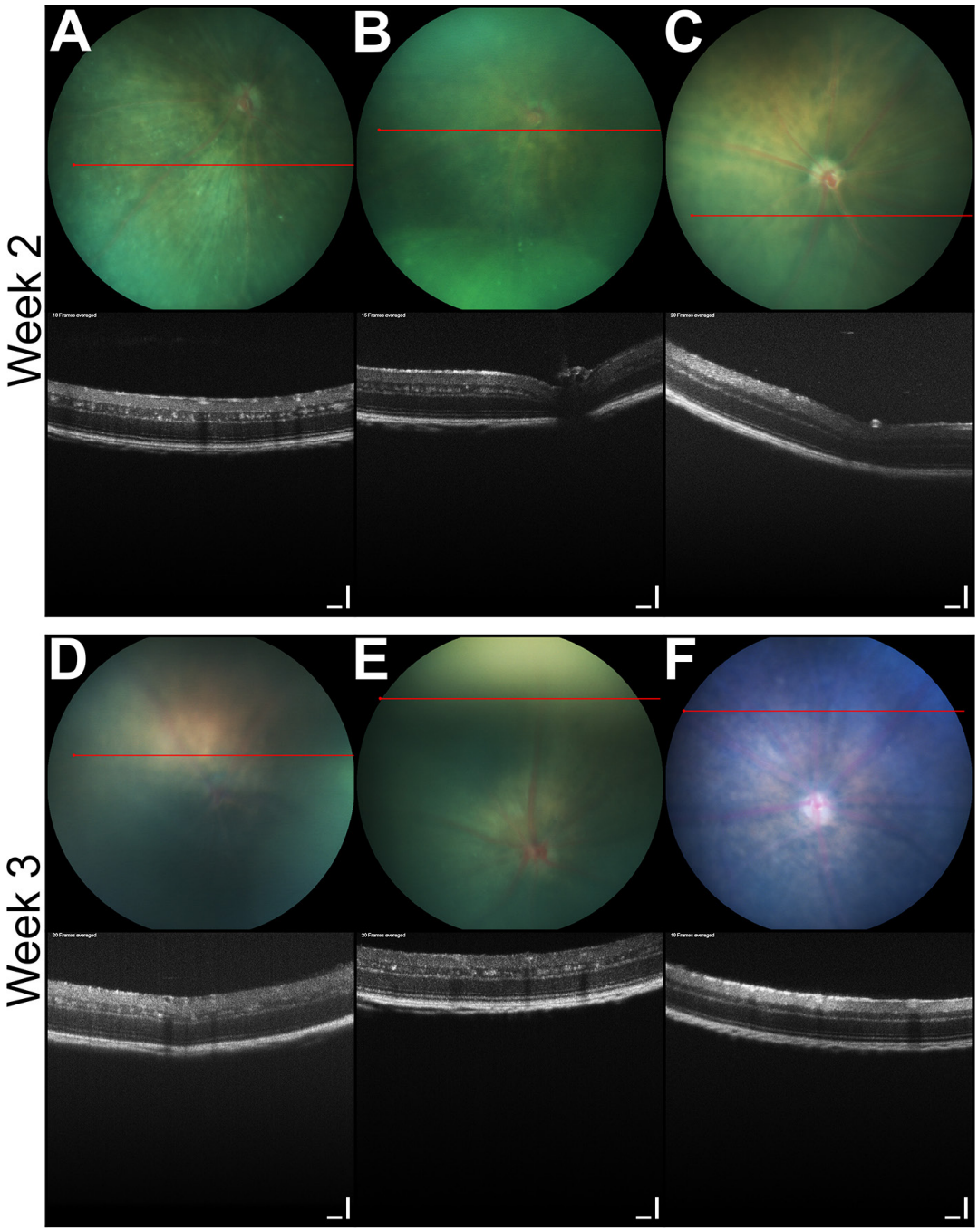

Figure 1. Earliest areas of T-antigen positive cells evident in TAg-RB retinas with OCT. At 2 (**A**, **B**) and 3 (**D**, **E**) weeks of age, hyperreflective clusters are seen in the inner nuclear layer of T-antigen retinoblastoma (TAg-RB) but not (**C**, **F**) wild-type eyes with optical coherence tomography (OCT) (bottom). All fundi appear normal at this age (top). OCT scale bars=100 µm.

human retinoblastoma [11,19-22]. Because of these features, this model has been used extensively for preclinical testing of retinoblastoma therapies and studies of genetic modifiers of disease progression [23].

Histology is the standard method for quantitative studies of retinal morphology and pathology of rodent models [24]. A major shortcoming of this technique is that a large number of animals are needed for each study since animals must be euthanized at each time point required. Because each animal provides only a single data point, studying disease progression over time is challenging. Thus, novel methods of monitoring tumor growth in these models are required.

Ocular optical coherence tomography (OCT) is one such method. It has taken on an important role in human ophthalmic practice, including retinoblastoma management. In particular, in the clinic, OCT has enabled precise anatomic findings, such as demarcating intratumoral cysts [25], viewing of the macula behind vitreous seeds [26], and identifying small tumors and documenting the middle-retinal layer origin of these lesions [27]. By assessing retinal morphology, OCT also helps determine reasons for visual loss post-treatment [28] and prognostication of visual potential after treatment [29]. OCT is especially effective for documenting response to therapy [30].

OCT has also been used in animal retinoblastoma models. We have used OCT for rapid, non-invasive, in vivo ascertainment of retinoblastoma xenografts in the newborn rat model [31]. OCT has been used to detect tumors in utero in the Pax6-SV40 TAg mouse model [32], and has previously been applied to characterize TAg-RB tumors. First, a single tumor was imaged, and its volume estimated in a 9-week-old TAg-RB mouse [33]; then this approach was expanded to quantify growth over time in 10- to 14-week-old mice [34]. Using an automated segmentation algorithm, response to an antiangiogenic treatment in this model was monitored with OCT [35,36]. However, these prior studies did not follow tumor growth over an extended time period.

Here, we evaluated whether OCT imaging could be used to document tumor growth in the TAg-RB model from the earliest stages of tumor development up to vitreous-filling tumors (a 5-month period). Although blockade of tumor initiation in a patient predisposed to retinoblastoma is a potential

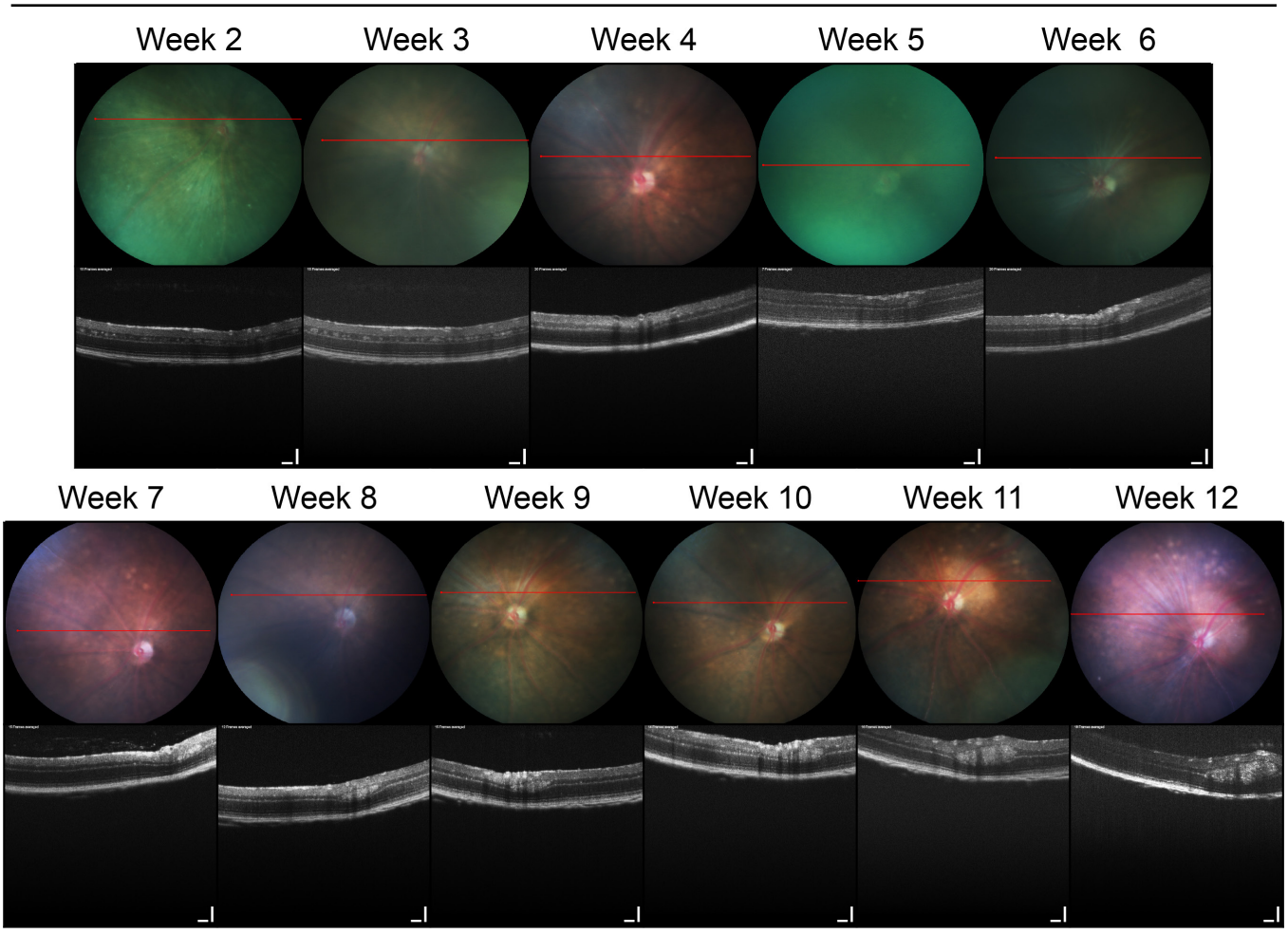

Figure 2. Longitudinal imaging of a TAg-RB tumor with OCT. A single, representative eye imaged weekly from 2 to 12 weeks of age as indicated shows early clusters of presumptive T-antigen (TAg)-positive cells decreasing around 4 weeks, as previously observed with immunohistochemistry. Then, a distinct tumor mass is first evident at 5 weeks and grows over subsequent weeks. Retinal blood vessels (seen by their shadow) sit adjacent to this small tumor during weeks 6–7 and atop the tumor from week 8. Optical coherence tomography (OCT) scale bars=100 µm.

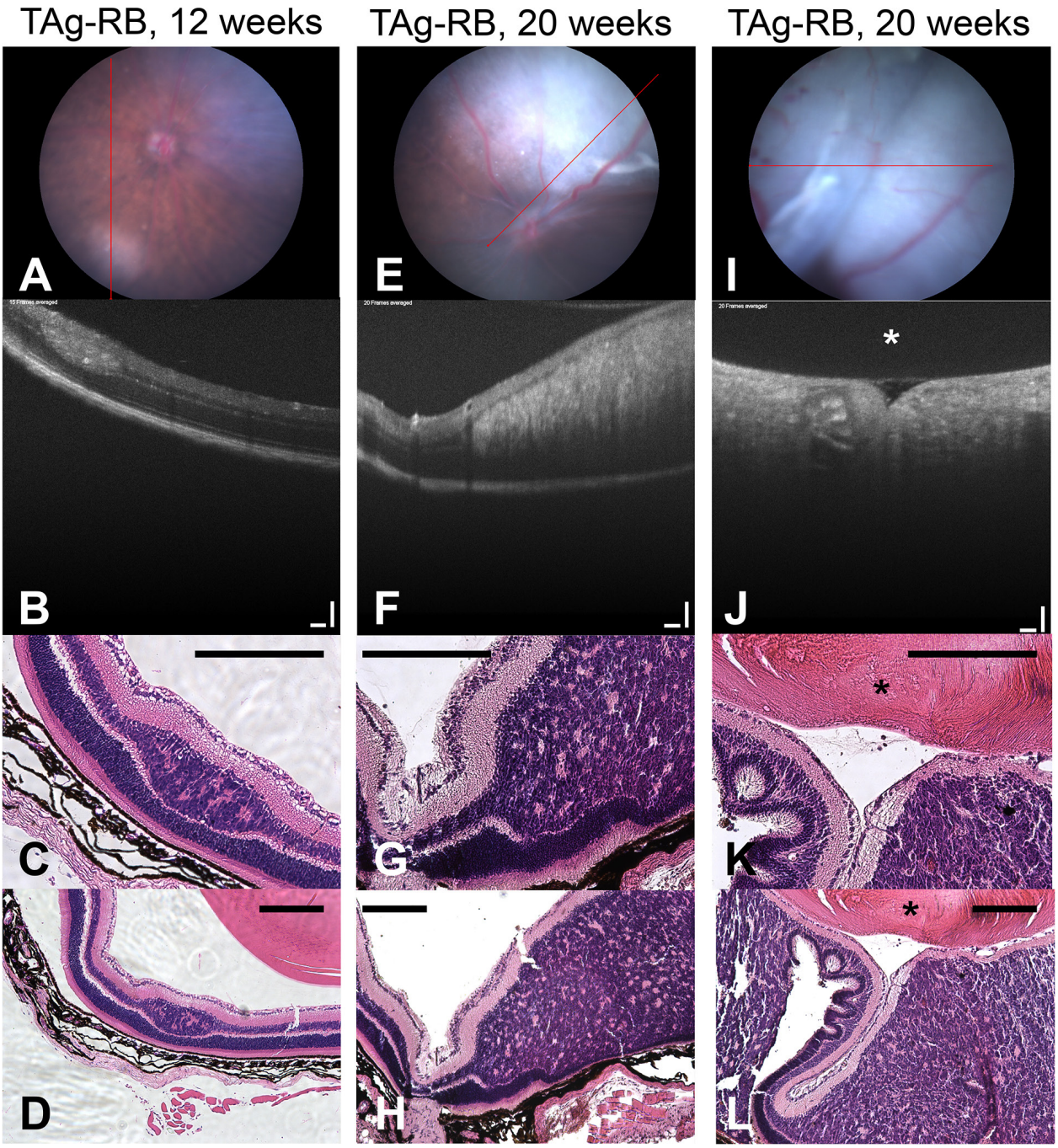

Figure 3. Histology validates OCT findings. Examples of a 12-week and two 20-week T-antigen retinoblastoma (TAg-RB) eyes analyzed with funduscopy (**A**, **E**, **I**); optical coherence tomography (OCT) (**B**, **F**, **J**), OCT scale bars=100 µm; high-magnification hematoxylin and eosin (H&E; **C**, **G**, **K**); and low-magnification H&E (**D**, **H**, **L**), scale bars=200 µm. The lens is indicated with an asterisk (*).

point of therapeutic intervention, in vivo imaging of the first weeks of tumor growth in a retinoblastoma animal model has not been performed previously. By using OCT for in vivo monitoring of tumor growth, we add to the understanding of retinoblastoma tumorigenesis in this model, as well as open up new avenues for investigating potential treatments.

METHODS

Animals: All animal experiments were approved by the Indiana University School of Medicine Institutional Animal Care and Use Committee (Protocol 10521) and adhered to all standards set forth in the ARVO Statement for the Use of Animals in Ophthalmic and Visual Research. TAg-RB mice on a C57BL/6 background (formally, CB6-Tg(TagRb)1Plm/Mmjax) were obtained from the Mutant Mouse Regional Resource Center at the Jackson Laboratory (Bar Harbor, ME; catalog number 032031) and bred in-house. Transgenic mice were bred with wild-type littermates to ensure hemizygosity. Mice were housed on a 12 h:12 h light-dark cycle (lights on at 0700) with access to food and water ad libitum. Pups were weaned at 3–4 weeks of age.

Genotyping: Ear punches were taken at time of weaning and processed for genotyping with the REDExtract-N-Amp Tissue kit (Sigma, St. Louis, MO) according to the manufacturer's instructions, with primer concentrations of 250 nM each and annealing at 58 °C. The primers used were TAg transgene [37], forward 5′-GAC TTT GGA GGC TTC TGG GAT GCA ACT GAG-3′ and reverse 5′-GGC ATT CCA CCA CTG CTC CCA TTC ATC AGT-3′; and internal control *Fabpi* (PCR Genotyping Primer Pairs), forward 5′-TGG ACA GGA CTG GAC CTC TGC TTT CCT AGA-3′ and reverse 5′-TAG AGC TTT GCC ACA TCA CAG GTC ATT CAG-3′.

Imaging: Imaging of the animals began at 2 weeks of age, by which time mouse eyes have naturally opened. All animals were then imaged on a weekly basis, for at least 12 and up to 20 weeks, at which point large tumors caused protrusion of the eye, necessitating euthanasia. Image-guided OCT and bright-field imaging using a Micron III intraocular imager (Phoenix Research Labs; Pleasanton, CA) was performed as described [31], with the following modification: Anesthesia was induced with a mixture of dexmedetomidine (0.5 mg/kg) and ketamine (50 mg/kg), with atipamezole reversal (5 mg/kg).

Histopathology: After the imaging protocols were completed at 12 and 20 weeks, the animals were overdosed with inhaled isoflurane and underwent cervical dislocation, and the eyes were removed for preservation. Each eye was fixed in 4% paraformaldehyde overnight and then transferred to a 70% ethanol solution. Whole eyes were embedded in paraffin, and 5- to 7-µm sections were obtained using a microtome. Mayer's hematoxylin and eosin staining was performed as described [31]. Bright-field micrographs were taken with an EVOS-fl digital microscope (AMG, Mill Creek, WA).

Statistical analysis: The distribution of intraretinal lesions between TAg-RB and wild-type animals was analyzed with Fisher's exact test, with a two-tailed p value <0.05 deemed significant.

RESULTS AND DISCUSSION

Earliest imaging of neoplasia in TAg-RB retinas: To profile the initiation of tumors in the TAg-RB model, we performed OCT and funduscopy at 2 and 3 weeks of age (Figure 1). At these time points, multiple small lesions were evident throughout the inner nuclear layer of both eyes of all TAg-RB mice (10/10 animals; 20/20 eyes). No lesions were present in the eyes of the wild-type mice (0/10; p=0.00001, Fisher's exact test). The fundi of all mice appeared normal. The hyperreflective clusters of cells visible on OCT in the transgenic mice likely correspond to the earliest TAg-positive cells we previously observed by immunofluorescence [11]. Such cells are first evident as single cells in the inner nuclear layer at P8, and form distinct clumps of TAg-positive cells by P13 that enlarge through to P21. It would be valuable to assess the retinas of TAg-RB mice with OCT at P8 to seek the individual TAg-positive cells, but this would require surgical opening of the eyelids, which could confound normal ocular development [31].

Longitudinal study of TAg-RB tumors: To document the growth of individual tumors, we imaged the eyes of these same mice weekly up to 12 weeks of age (Figure 2). The small, hyperreflective lesions seen throughout the retina at weeks 2 and 3 regressed between weeks 4 and 5. This is in keeping with our previous immunohistochemical findings indicating that a wave of apoptosis kills off most TAg-positive cells around 4 weeks of age [11]. By week 6, the first solid individual tumors were detectible with OCT and funduscopy. On OCT, these tumors began as ellipsoid, hyperreflective masses within the inner nuclear layer and were occasionally shadowed by overlying retinal blood vessels. Presumably, these tumors grew from isolated, early hyperreflective lesions as seen at weeks 2–3 that survived apoptosis between weeks 4–5. Funduscopic examination of these tumors revealed a pale circular mass that obscured the underlying pigmented choroid but was overlaid with retinal blood vessels, which is consistent with our OCT findings. Tumors were light-colored, remained intraretinal, and grew preferentially in the periphery.

Tumor burden at this stage ranged from one to four individual tumors per TAg-RB eye, but tumors in the far periphery may have been missed on exam due to the limitations of the OCT and fundus camera optics. Since TAg-RB tumors preferentially form in the periphery [38], this represents one weakness of analysis of this particular tumor model with OCT.

The tumors continued to increase in size at each weekly imaging session, and developed more irregular morphology over time. At 12 weeks, the tumors remained discrete ellipsoids (Figure 2 and Figure 3A, B). By 20 weeks, however, in many cases, the tumors had grown together, filling the vitreous by distorting the inner retina all the way to the posterior aspect of the lens (Figure 3E,F,I,J). Since proptosis was observed at this stage, the animals were euthanized for humane considerations.

Given the modest number of tumors per eye and clear vascular "landmarks" in the fundus images, finding each individual tumor at each imaging session for longitudinal, image-guided OCT analysis was relatively straightforward (Figure 2). Previously, an elaborate gimbal system was designed for reproducible positioning of animals for OCT [34]; we did not find such a system necessary to identify each tumor over multiple sessions. Further development of segmentation algorithms [36] for tumor volume estimation and automated three-dimensional (3D) scans will enable rapid, in vivo quantification of individual tumor growth in future.

Comparison of OCT with histopathologic morphology: To validate our OCT findings, tumor morphology was confirmed with histological analysis at 12 and 20 weeks of age (Figure 3). At 12 weeks, well-defined, ellipsoid tumors showed an intralesional granularity on OCT not previously documented (Figure 3B) [33-36], likely due to the high resolution of the imaging system we used compared with those in earlier work. Comparison with histology suggested that this granularity was due to the Flexner-Wintersteiner and Homer Wright rosettes within these tumors (Figure 3C,D), although higher-resolution OCT is required to confirm this. In addition, at this stage, histology confirmed the inner nuclear layer location of these tumors as seen with OCT, with moderate distortion of the inner retina and more pronounced depression of the outer nuclear layer (Figure 3C,D).

Importantly, these small tumors bore a striking resemblance on OCT to those recently observed in human patients [27]. An inner nuclear layer origin, defined ellipsoid shape, some intralesional granularity, supratumoral retinal blood vessels, and depression of the outer nuclear layer were all shared features. One noticeable difference was that the human tumors appeared to distort the inner retinal layers more readily at a small size than the murine tumors, resulting in a more spherical shape than the ellipsoid murine tumors.

At 20 weeks, OCT showed massive intraretinal tumors distorting the inner retina all the way to the lens without disruption of the inner plexiform layer or the ganglion cell layer (Figure 3F,J); this was confirmed with histology (Figure 3G,H,K,L). The posterior aspect of these large lesions on OCT was shadowed by the tumor itself. However, retinal folds induced by these large tumors were seen on funduscopy (Figure 3I) and OCT (Figure 3J), which recapitulated closely what was subsequently observed with histology (Figure 3K,L).

Conclusions: Using OCT, we characterized abnormal growth in the TAg-RB model as early as 2 weeks of age, corresponding to the earliest stages at which tumors are histologically evident [11], and before they are visible with funduscopy. Further, OCT imaging determines the intraretinal location of tumors more easily and more precisely than funduscopy. Such early imaging will be useful for documenting the efficacy of chemopreventative approaches for retinoblastoma in this model [39]. Moreover, non-invasive tracking of tumor growth from its earliest stages as done here will allow better analysis of the efficacy of novel therapeutics tested in this powerful mouse model. It will also expand the time points readily assessable in genetic studies of the effect of retinoblastoma oncogenes and tumor suppressors on TAg-RB development [37,40].

ACKNOWLEDGMENTS

We thank Pamela I. Rogers and Keith Condon for assistance with histopathology, and Helen Dimaras and Brian Samuels for comments on the manuscript. This work was supported by American Cancer Society Institutional Research Grant IRG-84–002–28, an unrestricted grant from Research to Prevent Blindness, Inc., and a contract from Phoenix Research Labs. TWC is supported by NIH NCATS KL2TR001106. This work was previously presented in part at the Association for Research in Vision and Ophthalmology Annual Meeting, May 2014. TWC has received research and travel support from Phoenix Research Labs.

REFERENCES

1. Dimaras H, Kimani K, Dimba EA, Gronsdahl P, White A, Chan HS, Gallie BL. Retinoblastoma. Lancet 2012; 379:1436-46. [PMID: 22414599].

2. Abramson DH. Retinoblastoma: saving life with vision. Annu Rev Med 2014; 65:171-84. [PMID: 24422571].

3. Grossniklaus HE. Retinoblastoma. Fifty Years of Progress. The LXXI Edward Jackson Memorial Lecture. Am J Ophthalmol 2014; 158:875-91. [PMID: 25065496].
4. Shields CL, Lally SE, Leahey AM, Jabbour PM, Caywood EH, Schwendeman R, Shields JA. Targeted retinoblastoma management: when to use intravenous, intra-arterial, periocular, and intravitreal chemotherapy. Curr Opin Ophthalmol 2014; 25:374-85. [PMID: 25014750].
5. Sachdeva UM, O'Brien JM. Understanding pRb: toward the necessary development of targeted treatments for retinoblastoma. J Clin Invest 2012; 122:425-34. [PMID: 22293180].
6. Basavarajappa HD, Corson TW. KIF14 as an oncogene in retinoblastoma: a target for novel therapeutics? Future Med Chem 2012; 4:2149-52. [PMID: 23190103].
7. Zhang J, Benavente CA, McEvoy J, Flores-Otero J, Ding L, Chen X, Ulyanov A, Wu G, Wilson M, Wang J, Brennan R, Rusch M, Manning AL, Ma J, Easton J, Shurtleff S, Mullighan C, Pounds S, Mukatira S, Gupta P, Neale G, Zhao D, Lu C, Fulton RS, Fulton LL, Hong X, Dooling DJ, Ochoa K, Naeve C, Dyson NJ, Mardis ER, Bahrami A, Ellison D, Wilson RK, Downing JR, Dyer MA. A novel retinoblastoma therapy from genomic and epigenetic analyses. Nature 2012; 481:329-34. [PMID: 22237022].
8. Thériault BL, Dimaras H, Gallie BL, Corson TW. The genomic landscape of retinoblastoma: a review. Clin Experiment Ophthalmol 2014; 42:33-52. [PMID: 24433356].
9. Pacal M, Bremner R. Insights from animal models on the origins and progression of retinoblastoma. Curr Mol Med 2006; 6:759-81. [PMID: 17100602].
10. Windle JJ, Albert DM, O'Brien JM, Marcus DM, Disteche CM, Bernards R, Mellon PL. Retinoblastoma in transgenic mice. Nature 1990; 343:665-9. [PMID: 1689463].
11. Pajovic S, Corson TW, Spencer C, Dimaras H, Orlic-Milacic M, Marchong MN, To KH, Theriault B, Auspitz M, Gallie BL. The TAg-RB murine retinoblastoma cell of origin has immunohistochemical features of differentiated Müller glia with progenitor properties. Invest Ophthalmol Vis Sci 2011; 52:7618-24. [PMID: 21862643].
12. Rushlow DE, Mol BM, Kennett JY, Yee S, Pajovic S, Thériault BL, Prigoda-Lee NL, Spencer C, Dimaras H, Corson TW, Pang R, Massey C, Godbout R, Jiang Z, Zacksenhaus E, Paton K, Moll AC, Houdayer C, Raizis A, Halliday W, Lam WL, Boutros PC, Lohmann D, Dorsman JC, Gallie BL. Characterisation of retinoblastomas without *RB1* mutations: genomic, gene expression, and clinical studies. Lancet Oncol 2013; 14:327-34. [PMID: 23498719].
13. Dunn JM, Phillips RA, Becker AJ, Gallie BL. Identification of germline and somatic mutations affecting the retinoblastoma gene. Science 1988; 241:1797-800. [PMID: 3175621].
14. Friend SH, Bernards R, Rogelj S, Weinberg RA, Rapaport JM, Albert DM, Dryja TP. A human DNA segment with properties of the gene that predisposes to retinoblastoma and osteosarcoma. Nature 1986; 323:643-6. [PMID: 2877398].
15. Lee WH, Shew JY, Hong FD, Sery TW, Donoso LA, Young LJ, Bookstein R, Lee EY. The retinoblastoma susceptibility gene encodes a nuclear phosphoprotein associated with DNA binding activity. Nature 1987; 329:642-5. [PMID: 3657987].
16. Cheng J, DeCaprio JA, Fluck MM, Schaffhausen BS. Cellular transformation by Simian Virus 40 and Murine Polyoma Virus T antigens. Semin Cancer Biol 2009; 19:218-28. [PMID: 19505649].
17. Sáenz Robles MT, Pipas JM. T antigen transgenic mouse models. Semin Cancer Biol 2009; 19:229-35. [PMID: 19505650].
18. Eagle RC Jr. The pathology of ocular cancer. Eye (Lond) 2013; 27:128-36. [PMID: 23154492].
19. Dimaras H, Coburn B, Pajovic S, Gallie BL. Loss of p75 neurotrophin receptor expression accompanies malignant progression to human and murine retinoblastoma. Mol Carcinog 2006; 45:333-43. [PMID: 16555252].
20. Marchong MN, Chen D, Corson TW, Lee C, Harmandayan M, Bowles E, Chen N, Gallie BL. Minimal 16q genomic loss implicates cadherin-11 in retinoblastoma. Mol Cancer Res 2004; 2:495-503. [PMID: 15383628].
21. Orlic M, Spencer CE, Wang L, Gallie BL. Expression analysis of 6p22 genomic gain in retinoblastoma. Genes Chromosomes Cancer 2006; 45:72-82. [PMID: 16180235].
22. Houston SK, Piña Y, Clarke J, Koru-Sengul T, Scott WK, Nathanson L, Schefler AC, Murray TG. Regional and temporal differences in gene expression of LH_{BETA} T_{AG} retinoblastoma tumors. Invest Ophthalmol Vis Sci 2011; 52:5359-68. [PMID: 21571674].
23. Nair RM, Kaliki S, Vemuganti GK. Animal models in retinoblastoma research. Saudi J Ophthalmol 2013; 27:141-6. [PMID: 24227978].
24. Dimaras H, Marchong MN, Gallie BL. Quantitative analysis of tumor size in a murine model of retinoblastoma. Ophthalmic Genet 2009; 30:84-90. [PMID: 19373679].
25. Shields CL, Mashayekhi A, Luo CK, Materin MA, Shields JA. Optical coherence tomography in children: analysis of 44 eyes with intraocular tumors and simulating conditions. J Pediatr Ophthalmol Strabismus 2004; 41:338-44. [PMID: 15609518].
26. Hasanreisoglu M, Dolz-Marco R, Ferenczy SR, Shields JA, Shields CL. Spectral domain optical coherence tomography reveals hidden fovea beneath extensive vitreous seeding from retinoblastoma. Retina 2015; In press[PMID: 25756924].
27. Rootman DB, Gonzalez E, Mallipatna A, Vandenhoven C, Hampton L, Dimaras H, Chan HS, Gallie BL, Heon E. Hand-held high-resolution spectral domain optical coherence tomography in retinoblastoma: clinical and morphologic considerations. Br J Ophthalmol 2013; 97:59-65. [PMID: 23104902].
28. Shields CL, Materin MA, Shields JA. Review of optical coherence tomography for intraocular tumors. Curr Opin Ophthalmol 2005; 16:141-54. [PMID: 15870570].

29. Cao C, Markovitz M, Ferenczy S, Shields CL. Hand-held spectral-domain optical coherence tomography of small macular retinoblastoma in infants before and after chemotherapy. J Pediatr Ophthalmol Strabismus 2014; 51:230-4.

30. Shields CL, Pellegrini M, Ferenczy SR, Shields JA. Enhanced depth imaging optical coherence tomography of intraocular tumors: from placid to seasick to rock and rolling topography–the 2013 Francesco Orzalesi Lecture. Retina 2014; 34:1495-512. [PMID: 25014847].

31. Corson TW, Samuels BC, Wenzel AA, Geary AJ, Riley AA, McCarthy BP, Hanenberg H, Bailey BJ, Rogers PI, Pollok KE, Rajashekhar G, Territo PR. Multimodality imaging methods for assessing retinoblastoma orthotopic xenograft growth and development. PLoS ONE 2014; 9:e99036 [PMID: 24901248].

32. Larina IV, Syed SH, Sudheendran N, Overbeek PA, Dickinson ME, Larin KV. Optical coherence tomography for live phenotypic analysis of embryonic ocular structures in mouse models. J Biomed Opt 2012; 17:081410-1. [PMID: 23224171].

33. Ruggeri M, Wehbe H, Jiao S, Gregori G, Jockovich ME, Hackam A, Duan Y, Puliafito CA. In vivo three-dimensional high-resolution imaging of rodent retina with spectral-domain optical coherence tomography. Invest Ophthalmol Vis Sci 2007; 48:1808-14. [PMID: 17389515].

34. Ruggeri M, Wehbe H, Tsechpenakis G, Jiao SL, Jockovich ME, Cebulla C, Hernandez E, Murray TG, Puliafito CA. Quantitative evaluation of retinal tumor volume in mouse model of retinoblastoma by using ultra high-resolution optical coherence tomography. J Innov Opt Health Sci 2008; 1:17-28.

35. Cebulla CM, Jockovich ME, Boutrid H, Piña Y, Ruggeri M, Jiao S, Bhattacharya SK, Feuer WJ, Murray TG. Lack of effect of SU1498, an inhibitor of vascular endothelial growth factor receptor-2, in a transgenic murine model of retinoblastoma. Open Ophthalmol J 2008; 2:62-7. [PMID: 19517030].

36. Ruggeri M, Tsechpenakis G, Jiao S, Jockovich ME, Cebulla C, Hernandez E, Murray TG, Puliafito CA. Retinal tumor imaging and volume quantification in mouse model using spectral-domain optical coherence tomography. Opt Express 2009; 17:4074-83. [PMID: 19259247].

37. Marchong MN, Yurkowski C, Ma C, Spencer C, Pajovic S, Gallie BL. *Cdh11* acts as a tumor suppressor in a murine retinoblastoma model by facilitating tumor cell death. PLoS Genet 2010; 6:e1000923 [PMID: 20421947].

38. Kivelä T, Virtanen I, Marcus DM, O'Brien JM, Carpenter JL, Brauner E, Tarkkanen A, Albert DM. Neuronal and glial properties of a murine transgenic retinoblastoma model. Am J Pathol 1991; 138:1135-48. [PMID: 1708946].

39. Sangwan M, McCurdy SR, Livne-Bar I, Ahmad M, Wrana JL, Chen D, Bremner R. Established and new mouse models reveal *E2f1* and *Cdk2* dependency of retinoblastoma, and expose effective strategies to block tumor initiation. Oncogene 2012; 31:5019-28. [PMID: 22286767].

40. Dimaras H, Gallie BL. The $p75^{NTR}$ neurotrophin receptor is a tumor suppressor in human and murine retinoblastoma development. Int J Cancer 2008; 122:2023-9. [PMID: 18196575].

Articles are provided courtesy of Emory University and the Zhongshan Ophthalmic Center, Sun Yat-sen University, P.R. China. The print version of this article was created on 1 May 2015. This reflects all typographical corrections and errata to the article through that date. Details of any changes may be found in the online version of the article.